Thermal Comfort Measurement using Thermal-Depth Images for Robotic Monitoring

Jun Miura*, Mitsuhiro Demura, Kaichiro Nishi, and Shuji Oishi

Department of Computer Science and Engineering, Toyohashi University of Technology
Toyohashi, Aichi 441-8580, Japan

Abstract

This paper describes an application of thermal-depth images to human thermal comfort measurement. A mobile monitoring of the elderly and residents of care houses is one of the promising applications of mobile assistive robots. Monitoring if a person feels comfortable is an important task of such robots. We rely on an established comfort measure in the architecture domain, namely, *predicted mean vote* (PMV). PMV is calculated mainly by six factors and one of which is the clothing insulation or clo-value. Clo-values are usually measured by a thermal mannequin, a specially-designed apparatus for the purpose. We apply human recognition techniques in thermal-depth images to efficiently measure clo-values, thereby enabling on-line assessment of thermal comfort. We evaluate the method and develop a mobile robot system for experimental testing.

Keywords: Thermal comfort measurement, thermal-depth images, clothing insulation, mobile assistive robot.

1. Introduction

Service robots are expected to support our daily life in the near future with the continuous development of robotics technologies. As we are facing the *aged society*, one promising application is *robotic monitoring*, in which a robot lives with and takes care of the elderly who live alone.

Monitoring people has been dealt with in robotics and computer vision domains. One popular approach is so-called *smart house* [1, 2, 3] which uses many embedded cameras and sensors, usually put on ceilings and walls, to monitor the state and the activity of residents inside. Recent IoT (Internet of Things) technologies have also been contributing to this line of research and development. Since such an approach requires pre-installed sensors, it is sometimes difficult to apply to existing houses. Another approach is to use wearable devices such as a thermometer and a cardiometer for health monitoring [4]. Using such devices makes it possible to take direct and reliable data in real-time, but may impose a physical and/or mental burden on people.

One of the monitoring tasks is to examine if a resident is in a comfortable state. Such a comfort depends on various factors but they can be divided into two main factors. One is how a residence is in a good condition [5, 6], that is, for example, whether temperature, illuminance, or air cleanness are in good condition. The other is how residents themselves in a state of good health. Some combined effects of such factors will determine the comfort of the resident. This paper deals with *thermal comfort*, which measures human satisfaction with the thermal environment [7]. We use PMV (predicted mean vote) as a measure and develop a robot system for PMV measurement.

The sensory data we choose for measuring thermal comfort is thermal-depth image, since usual RGB images sometimes suffer from privacy issues as well as sensitivity to illumination conditions. By using a thermal camera in addition to a depth one, we can effectively segment human regions and calculate thermal comfort measures. The contributions of the research are: (1) to propose an approach to mobile robot-based thermal comfort measurement, and (2) to develop an experimental system and to validate the proposed methods. This paper is an extended version of robotic thermal comfort measurement described as a part of our previous paper [8]. The most significant part of this paper compared with [8] is the experimental verification of thermal image-based estimation of clothing insulation and thermal comfort.

The rest of the paper is organized as follows. Section 2 describes related work. Section 3 explains our robot system for mobile thermal comfort measurement. Section 4 explains the measure of thermal comfort in detail and methods of calculating necessary factors including the clothing insulation. Section 5 shows experimental results for evaluating thermal comfort measurements and for robotic monitoring. Section 6 discusses the use of the system in actual robotic monitoring scenarios as well as possible improvements of the proposed methods. Section 7 summarizes the paper.

*Corresponding author

2. Related Work

2.1. Thermal comfort measurement

PMV is one of the most popular thermal comfort measures and mainly depends on four environmental factors (air temperature, mean radiant temperature, air velocity, and relative humidity) and two personal factors (clothing insulation and activity level) [5]. In the architecture domain, these factors are usually measured using special devices and/or a specially installed set of (fixed) sensors [9].

For measuring and estimating environmental factors, using a robot as a mobile base is a promising approach. Previous researches deal with various applications such as odor map making [10], gas leak position localization [11], temperature and illuminance distribution mapping [12].

The activity level of a person is related to their metabolic rate and thus to the thermal comfort. The relationships between the metabolic rate and various activities such as seating, standing, and cooking have been analyzed [7]. Therefore activity recognition techniques (e.g., [13, 14]) could be adopted for thermal comfort measurement in robotic monitoring.

The clothing insulation, which is the other personal factor, is usually measured using a thermal mannequin [7]. The clothing insulation for various materials and designs have also been compiled in a database, which can be used for an on-line thermal comfort measurement. Matsumoto et al. [15] presented a method of measuring thermal comfort using the visual recognition of the material and the weight of clothing.

Several methods have been proposed for thermal comfort measurement without estimating the clothing insulation. Ranjan and Scott [16] proposed a method of detecting and predicting thermal comfort by looking for physiological markers of vasodilation and vasoconstriction in thermal images. Metzmacher et al. [17] developed a method of thermal comfort measurement using a thermal camera and a numeral human heat transfer model, enabling measuring thermal comfort in occluded local body regions.

2.2. Thermal-depth image generation

Combination of thermal and depth images has recently been widely used for various applications such as people detection and disaster response. Using two kinds of cameras entails a procedure for calibrating their relative pose (i.e., extrinsic parameters). We need calibration patterns which are visible from both types of cameras.

Rangel et al. [18] used a board with circular holes for a thermal-depth calibration. These holes can easily be detected by a depth camera, but could be difficult for a thermal cameras when a sufficient temperature difference does not exist between the board and the background. Rzeszotarski and Więcek [19] put aluminium sheets on white regions in a checker board for a thermal-RGB camera calibration. Aluminium sheets provide high reflection of infrared rays and are good for making markers for infrared cameras, but this approach cannot be applied to depth cameras. Oreifej et al. [20] describes a method of calibrating three modalities, an optical camera, a thermal camera, and a 3D LIDAR, based on optical-thermal and optical-LIDAR calibration.

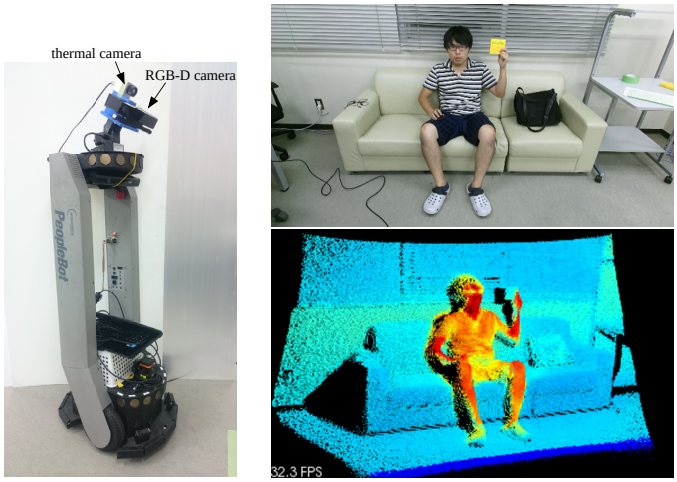

(a) Robot and cameras. (b) Test scene and thermal-depth data.

Figure 1: Robot and an example thermal-depth data.

3. Thermal Comfort Monitoring Robot

Fig. 1(a) shows our monitoring robot prototype. The robot is quipped with a thermal camera and an RGB-D camera as well as thermal and humidity sensors. Fig. 1(b) shows an example of thermal-depth data, viewed from a different viewpoint from the original.

3.1. Thermal-depth calibration

We use PI-160 (Optris, 160 × 120 pixels) and Kinect v2 (Microsoft) as a thermal and a depth camera, respectively. Since it is difficult to make a calibration board which is visible from both cameras, we additionally use an RGB camera of Kinect v2 and calculate the relative pose between the thermal and the depth camera from those of the thermal-RGB and the RGB-depth camera pair. As a result, we use different calibration boards for each pair.

A popular checker board is used for the RGB-depth calibration, because the depth camera of Kinect v2 can also produce NIR (near infrared) images, in which the board is sufficiently visible. Fig. 2 shows images of the board in both camera images.

For the thermal-RGB calibration, we follow the work by Rzeszotarski and Więcek [19]. In addition to putting aluminium sheets on white regions, we heat up the board to make the temperature difference clearer for the thermal camera. Fig. 3 shows images of the board, which are visible by both the RGB and the thermal camera. Note that this aluminium-pasted board is difficult to be properly observed in NIR images, and therefore we cannot directly calibrate the thermal-depth camera pair using this board.

(a) RGB image.

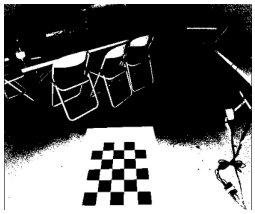

(b) NIR image.

Figure 2: Calibration board captured by the RGB and the NIR camera.

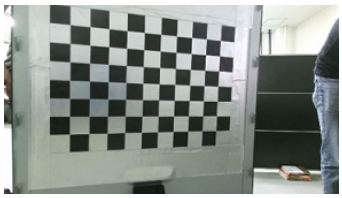

(a) RGB image.

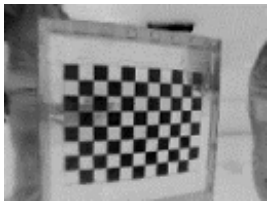

(b) Thermal image.

Figure 3: Calibration board captured by the RGB and the thermal camera.

(a) Scene.

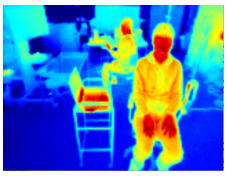

(b) Thermal image.

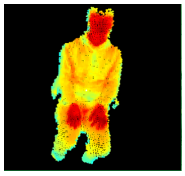

(c) Human region.

Figure 4: Human detection using thermal point cloud.

From both calibration results, we indirectly calculate the thermal-depth calibration. As shown in Fig. 1(b), a consistent thermal point cloud is obtained from an example of thermal-depth data, indicating that the calibration works reasonably well.

3.2. Human region extraction

Thermal-depth images are useful for extracting human regions in a complex background. We use a combination of a thermal-based thresholding and a depth-based Euclidean distance clustering for human region extraction [8]. We set a temperature threshold to 23[°C] for human region detection, and that for clustering is set to 80[mm]. A size filtering is then adopted to extract only the points of the humans. Fig. 4 shows a human detection result. In the thermal image, since there are many warm regions and some of them are connected to the front human region, human detection using only thermal image may fail. By using the thermal point cloud, the human region is correctly extracted.

3.3. Temperature measurement of the environment

The robot uses three thermal sensors (thermocouples) for measuring temperatures at three different heights. In the architecture domain, guidelines are set for temperature measurements. According to such guidelines (e.g., [21]), the measured position is the center of the floor in the space and its height is 100[cm], and it is desirable to additionally measure the temperature at the heights of 10[cm] and 60[cm] when sitting and 10[cm] and 170[cm] when standing. Considering both the requirement in architecture and the robot structure, the thermocouples are set at the heights of 10[cm], 70[cm], and 170[cm].

Table 1: PMV and thermal sensation scale.

PMV	Thermal Sensation Scale
+3	hot
+2	warm
+1	slightly warm
0	neutral
-1	slightly cool
-2	cool
-3	cold

4. Thermal Comfort Measurement

4.1. Predicted mean vote

Thermal comfort is human satisfaction with the thermal environment and influenced by various factors such as physical, physiological, psychological processes. One of the indices of assessing thermal comfort is PMV (predicted mean vote), which is determined in ISO 7730 [22]. This is an index that predicts the mean value of the votes of a large group of persons on the 7-point *thermal sensation scale* (see Table 1), based on the heat balance of the human body between the internal heat production in the body and the loss of heat to the environment. PPD (predicted percentage of dissatisfied) is also used as another measure, which quantitatively predicts the percentage of thermally dissatisfied people who feel too cool or too warm.

PMV basically depends on the following six factors [7]: thermal insulation (or thermal resistance) of clothing (called *clo-value*), activity level (met-value), air temperature, air velocity, radiant temperature, and humidity. Among these, the air temperature and the humidity are measured by on-robot sensors. The radiant temperature is assumed to be the same as the air temperature. The air velocity is set to be a small value for indoor environments. The activity level is determined based on human posture, such as sitting and standing, and actions taken. The clo-value can approximately be measured using thermal images as explained below.

4.2. Estimating clo-value

4.2.1. Calculation of clo-value

The clo-value of clothing is usually measured on a thermal mannequin, but that cannot be used for on-line measurements in a daily situation. We instead adopt an estimation method based on thermal measurements. The

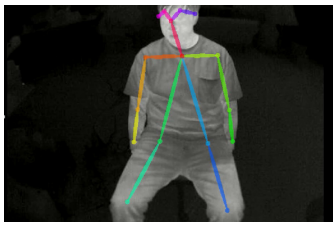

Skeleton extraction

Clothing region extraction

(a) Sitting.

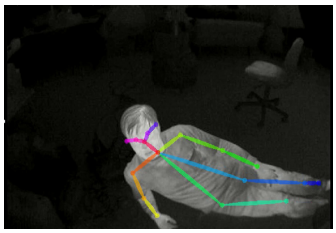

Skeleton extraction

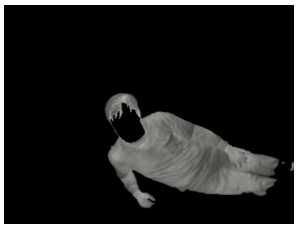

Clothing region extraction

(b) Lying.

Figure 5: Clothing region extraction.

clo-value I_{clo} is given by [23]:

$$I_{clo} = \frac{1}{0.155 \cdot h} \frac{t_s - t_{cl}}{t_{cl} - t_o}, \tag{1}$$

where h is the heat transfer coefficient of the human body (set to 8.6 assuming a calm indoor environment [24]), t_o is the operative temperature (approximated here by the air temperature), t_s is the skin surface temperature, and t_{cl} is the clothing surface temperature. The last two temperature values are measured using thermal images as follows.

4.2.2. Extracting skin and clothing regions in the thermal image

A human region extracted in thermal-depth images (see Sec. 3.2) is then divided into skin and clothing regions. We use the *GrabCut* [25] algorithm for this division. Since the algorithm requires seed points, we extract them with a simple assumption that the face is exposed and shoulders are covered by clothings. These joint positions are detected by using OpenPose [26]. Fig. 5 shows skeleton extraction and clothing region extraction for two cases (sitting and lying).

Once the skin and the clothing region are extracted, their average temperatures are used as the skin surface temperature (t_s) and the clothing surface temperature (t_{cl}) for calculating eq. (1). The averaged calculation time of clo-value is about 2.2[sec], which is fast enough for calculating the clo-values of people resting in a room.

4.3. Estimating activity level

Postures and activities can be determined by analyzing the human region in the image. The activity level, represented in *met*, is then determined by referring to a precalculated table [7]. The values are, for example, 1[met] for quiet sitting and 0.7[met] for sleeping.

(a) Experimental scene.

(b) Thermal image.

Figure 6: A thermal mannequin with a long-sleeved T-shirt

5. Experimental Results

5.1. Evaluation of clothing insulation measurement

Clo-values for typical clothing are suggested in the literature [7]. However, the details of materials and fabrications are different from one clothing to another and so are clo-values. We therefore compared the clo-value measurement using our thermal camera-based method and that by using a thermal mannequin.

We use three types of clothing, a long-sleeved T-shirt, the layers of that T-shirt and a cardigan, and the layers of the T-shirt and a fleece jacket. Fig. 6 shows a scene of the thermal mannequin wearing the T-shirt and its thermal image. The target temperature of the mannequin body is set to 33[°C] and that of the room is set to 22[°C]. Since the clo-value changes for each part of the body, we measure them for the following five positions, which are visible from our monitoring robot: chest, right and left upper arm, right and left forearm. We also use a region on the face for measuring skin surface temperature. We chose five pixels in the respective positions and calculated the averaged temperature for reducing the effect of pixel-wise noise.

Table 2 shows the results for the three types of clothing. The first and the second column of the tables are the temperature of clothing surface and skin surface, respectively. These values are measured by the thermal camera and used for estimating the clo-values. The error in temperature measurement of the thermal camera we used is specified as ±2[deg]. The measured temperatures of the skin surface are within this range from the target temperature (33[°C]).

The clo-values is separately measured by using the thermal mannequin from the target mannequin skin temperature, the measured air temperature, and the heat loss of the mannequin. Considering this meaurement as a target,

Table 3: Summary of clo-value comparison.

	averaged difference	standard deviation
single T-shirt	-0.15	0.17
T-shirt with cardigan	-0.34	0.26
T-shirt with fleece jacket	-0.95	0.65

Table 4: Summary of PMV comparison.

	averaged difference	standard deviation
foot height	-0.37	1.91
upper body height	-0.93	1.60
face height	-0.87	1.25

we examine the difference between the target clo-value and the one measured by our method.

The averaged differences and the standard deviations are summarized in Table 3. The tables show that the proposed method underestimates and that the absolute difference increases as the amount clothing increases. The reason of this tendency could be a complex air insulation between clothings, but further investigation is necessary. These differences are not very small but at least qualitatively acceptable considering the simplicity of the method.

We also analyze the effect of this difference on PMV. Let the clo-value be 0.5 in, for example, the case where PMV is -0.20 (between *normal* and *slightly* cool). When the real clo-value is larger by the maximum average difference (i.e., 0.95 in Table 3), PMV becomes 0.97 (slightly warm), being higher by 1.17.

5.2. Evaluation of PMV measurement

The next experiment is to evaluate the PMV measurement in comparison with subjective assessments. We set up three rooms with warm, normal, and cool temperature. Each subject spends for twenty minutes and takes questions. The questionnaire has three questions asking one of seven PMV scale (see Table 1) for three heights at foot-level, upper body-level, and face-level. We obtained data from five, seven, and five subjects for the warm, the normal, and the cool room, respectively.

Fig. 7 shows the plot of the relationship between the predicted and the subjective PMV values, indicating most of predictions are reasonable. The averaged differences and the standard deviations are summarized in Table 4. We then convert obtained PMV values into the seven classes using the midpoints of sensation values as thresholds. For example, a PMV value is classified as *normal* if its absolute value is less than 0.5, and classified as *warm* if it is between 1.5 and 2.5. Direct comparison of predicted and subjective classes results in the accuracy of 0.29, 0.29, and 0.35 for the foot, the upper body, and the face height, respectively. Since the maximum error of PMV due to that of clo-value is about one (see Sec. 5.1), if we allow the matches with neighboring classes, the accuracy values become 0.65, 0.71, and 0.65, respectively. This would be reasonable for being used for a robot to support, as we discuss later.

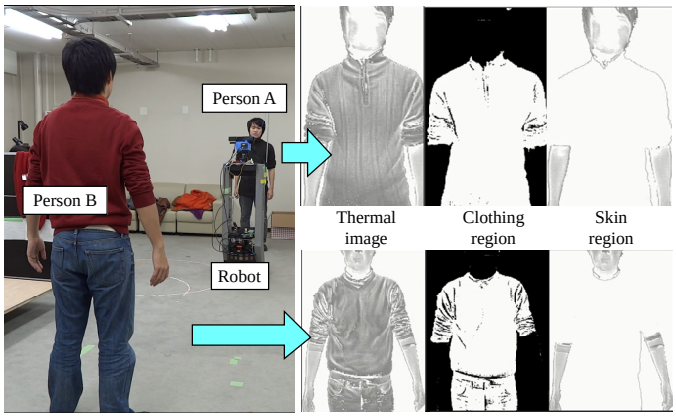

Figure 8: Thermal comfort measurement experiment.

Table 5: PMV measurement results.

Person	Clo-value	PMV (170cm)	PMV (110cm)	PMV (10cm)
A	0.21	-2.52	-2.86	-2.64
B	0.22	-2.43	-2.75	-2.54

5.3. Robot monitoring example

We implemented a capability of patrolling and monitoring thermal comfort on the robot, which is a combination of the proposed thermal comfort measurement method with navigation and human detection ones.

Fig. 8 shows an experimental scene. The robot patrols a designated area of a room, and when it finds a person, it moves to and takes a depth-thermal image of them, to calculate the clo-value, and then calculate PMV at three different heights (170[cm], 110[cm], and 10[cm] from the floor) to examine the thermal comfort at various body parts.

Table 5 summarizes the measurement results for the scene shown in Fig. 8. ISO 7730 describes that a comfortable environment has the PMV value in ± 0.5 [22]. The thermal environment of the experimental site is shown to be rather cool for both persons (see Table 1). To raise the lowest PMV value (-2.86) to be within the comfortable range (± 0.5), for example, the air temperature needs to be increased by nine degrees or the clo-value should be increased by 0.8 points. A monitoring robot could take an action such as turning on a heater or recommending to the respective person to layer another piece of clothing (e.g., sweater).

6. Discussion

PMV is a measure obtained through a complicated calculation of various factors, and is sometimes error-prone due to errors in estimating those factors. For example, our approach to estimating the clothing insulation is based simply on the temperature difference between the clothing and the skin surface. Although the obtained clo-values are

Table 2: Comparison of estimated clo-values for proposed and mannequin-based.

(a) long-sleeved T-shirt

	clothing surface temperature [°C]	skin surface temperature [°C]	heat loss of mannequin $[W/m^2]$	air temperature [°C]	clo-value (proposed)	clo-value (mannequin)
chest	30.8	33.3	57.3	21.3	0.20	0.55
right forearm	29.2	33.3	74.9	21.3	0.39	0.45
left forearm	27.7	33.3	73.4	21.3	0.65	0.51
right upper arm	30.9	33.3	76.2	21.3	0.19	0.42
left upper arm	30.2	33.3	67.3	21.3	0.26	0.53

(b) long-sleeved T-shirt and cardigan

	clothing surface temperature [°C]	skin surface temperature [°C]	heat loss of mannequin $[W/m^2]$	air temperature [°C]	clo-value (proposed)	clo-value (mannequin)
chest	29.9	35.0	40.4	21.3	0.45	1.09
right forearm	30.2	35.0	56.4	21.3	0.41	0.77
left forearm	27.8	35.0	59.0	21.3	0.83	0.75
right upper arm	28.7	35.0	41.8	21.3	0.64	1.23
left upper arm	27.2	35.0	42.6	21.3	1.00	1.17

(c) long-sleeved T-shirt and fleece jacket

	clothing surface temperature [°C]	skin surface temperature [°C]	heat loss of mannequin $[W/m^2]$	air temperature [°C]	clo-value (proposed)	clo-value (mannequin)
chest	27.8	33.7	25.3	21.3	0.69	2.18
right forearm	28.3	33.7	24.9	21.3	0.59	2.44
left forearm	26.6	33.7	46.1	21.3	1.03	1.10
right upper arm	26.7	33.7	31.3	21.3	1.00	1.81
left upper arm	27.2	33.7	38.2	21.3	0.85	1.36

qualitatively reasonable, we could consider a more complicated model (e.g., [27]). It would also be necessary to examine various combinations of clothings and environments. Air velocity at the position of a person is also difficult to precisely estimate from a mobile monitoring robot using on-board sensors.

Another drawback when applied to robotic monitoring is that the measure (i.e., PMV) is designed to predict the thermal sensation of most persons, not a specific individual. As a result, the PMV values are certainly effective for extreme cases (too cold or too hot), but provide only approximation. The proposed method seems to suffice in this sense. Further assessments will be, however, necessary for each person. One possible approach to this issue is to introduce an interaction and learning capability to the monitoring robot. By actively asking a person about their sensation and accumulating responses and/or observations of the person, the robot could make a model of the person's sensation which describes, for example, the mapping between the measured PMV value and the thermal sensation.

We currently use the Euclidean distance clustering for extracting a human region. Since the clustering performance has a large effect on the accuracy of the result, it is desirable to consider other clustering methods. As an extension of this work, we will apply weighted k-means clustering [28] and evaluate the results obtained by the proposed method with two different clustering methods.

7. Summary

Thermal comfort measurement is an important task of the robotic monitoring of residents. This paper has described a novel approach to thermal comfort measurement using a mobile robot. We use PMV as a measure of thermal comfort, which is calculated by six main factors; two personal and four environmental ones. We developed a method of estimating one of the personal factors, that is, the clothing insulation (or clo-value) using a depth-thermal camera system. A procedure for depth-thermal camera calibration is also developed. We evaluated the clothing insulation measurement using a thermal mannequin and the PMV measurement in comparison with a user questionnaire. The evaluation results show a certain level of accuracy that could be used for robotic monitoring. We finally discussed the use of the current system in actual situations as well as improving measurement accuracy.

Acknowledgment

The authors would like to thank Prof. Kazuyo Tsuzuki of Toyohashi University of Technology for her support in using the thermal mannequin. This work is in part supported by JSPS KAKENHI Grant Numbers 25280093/17H01799 and the Hibi Science Foundation.

References

[1] I. Mikic, K. Huang, M. Trivedi, Activity monitoring and summarization for an intelligent meeting room, in: Proceedings of IEEE Workshop on Human Motion, 2000.

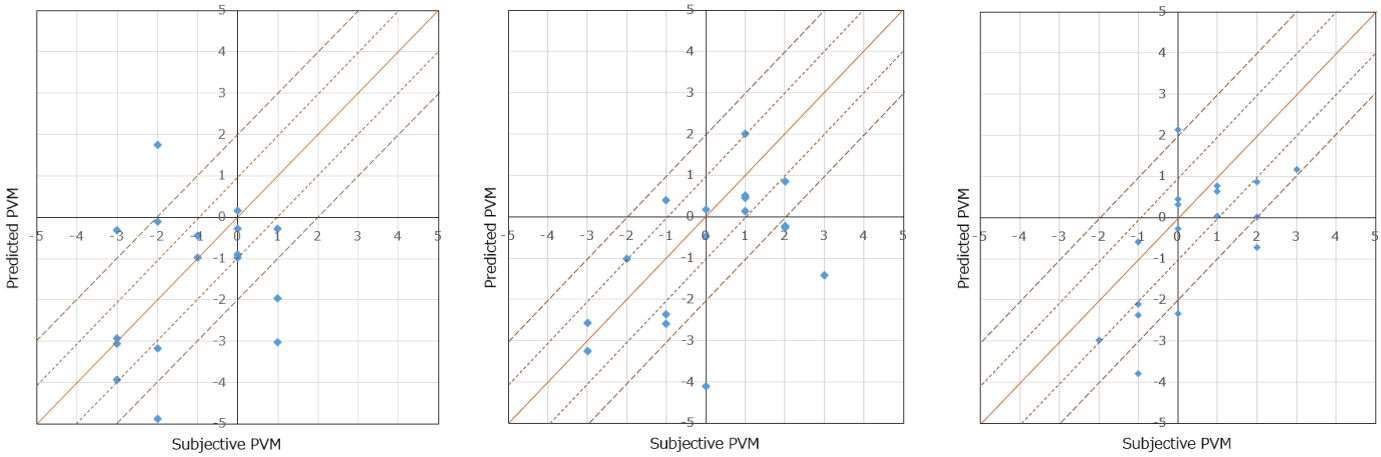

(a) foot height. (b) upper body height. (c) face height.

Figure 7: Comparison of predicted and subjective PMV's. The horizontal axis indicates the user's subjective assessment and the vertical axis indicates the predicted (measured) PMV by the proposed method.

[2] C. Wu, A. Khalili, H. Aghajan, Multiview activity recognition in smart homes with spario-temporal features, in: Proceedings of the 4th ACM/IEEE Int. Conf. on Distributed Smart Cameras, 2010, pp. 142–149.

[3] T. Mori, S. Tominaga, H. Noguchi, M. Shimoasaka, R. Fukui, T. Sato, Behavior prediction from trajectories in a house by estimating transition model using stay points, in: Proceedings of IEEE/RSJ Int. Conf. on Intelligent Robots and Systems, 2011, pp. 3419–3425.

[4] A. Pantelopoulos, N. Bourbakis, A survey on wearable sensor-based systems for health monitoring and prognosis, IEEE Trans. on Systems, Man, and Cybernetics Part C: Applications and Reviews 40 (1) (2010) 1–12.

[5] A. Melikov, Design and assessment of indoor environment, in: Proceedings of CLIMA 2000, 1997.

[6] D. Raimondo, S. Corgnati, B. Olesen, Evaluation methods for indoor environmental quality assessment according to EN15251, REHVA European HVAC J. 04/2012 (2012) 14–19.

[7] ASHRAE Handbook of Fundamentals, Americal Society of Heating, Refrigerating, and Air-Conditioning Engineers, 2009.

[8] K. Nishi, M. Demura, J. Miura, S. Oishi, Use of thermal point cloud for thermal comfort measurement and human pose estimation in robotic monitoring, in: Proceedings of 5th Int. Workshop on Assistive Computer Vision and Robotics, 2017.

[9] K. Fabbri, Thermal comfort evaluation in kindergarten: Pvm and ppd measurement through datalogger and questionnaire, Building and Environment 68 (2013) 202–214.

[10] L. Marques, A. Martins, A. de Almeida, Environmental monitoring with mobile robots, in: Proceedings of the 2005 IEEE/RSJ Int. Conf. on Intelligent Robots and Systems, 2005, pp. 3624–3629.

[11] V. H. Bennetts, A. Lilienthal, A. Khaliq, V. P. Sesé, M. Trincavelli, Towards real-world gas distribution mapping and leak localization using a mobile robot with 3d and remote gas sensing capabilities, in: Proceedings of 2013 IEEE Int. Conf. on Robotics and Automation, 2013, pp. 2327–2332.

[12] S. Kani, J. Miura, Mobile monitoring of physical states of indoor environments for personal support, in: Proceedings of 2015 IEEE/SICE Int. Symp. on System Integration, 2015, pp. 393–398.

[13] M. Tenorth, F. de la Torre, M. Beetz, Learning probability distributions over partially-ordered human everyday activities, in: Proceedings of 2013 IEEE Int. Conf. on Robotics and Automation, 2013, pp. 4539–4544.

[14] H. Koppula, R. Gupta, A. Saxena, Learning human activities and object affordances from rgb-d videos, Int. J. of Robotics Research 32 (8) (2013) 951–970.

[15] H. Matsumoto, Y. Iwai, H. Ishiguro, Estimation of thermal comfort by measuring clo value without contact, in: Proceedings of 2011 IAPR Conf. on Machine Vision Applications, 2011, pp. 491–494.

[16] J. Ranjan, J. Scott, ThermalSense: Determining Dynamic Thermal Comfort Preferences using Thermographic Imaging, in: Proceedings of 2016 ACM Int. Joint Conf. on Pervasive and Ubiquitous Computing, 2016, pp. 1212–1222.

[17] H. Metzmacher, D. Wölki, C. Schmidt, J. Frisch, C. van Treeck, Real-time Assessment of Human Thermal Comfort Using Image Recognition in Conjunction with a Detailed Numerical Human Model, in: Proceedings of Building Simulation 2017: 15th Conf. of IBPSA, 2017, pp. 691–700.

[18] J. Rangel, S. Soldan, A. Kroll, 3D thermal imaging: Fusion of thermography and depth cameras, in: Proceeings of 12th Int. Conf. on Quantitative InfraRed Thermography, 2014.

[19] D. Rzeszotarski, B. Więcek, An integrated thermal and visual camera system for 3d reconstruction, in: Proceedings of 11th Int. Conf. on Quantitative InfraRed Thermography, 2012.

[20] O. Oreifej, J. Cramer, A. Zakhor, Automatic generation of 3d thermal maps of building of interiors, ASHRAE trans. 120 (2).

[21] Architectural Institute of Japan, Academic Standards for Measurement of Indoor Thermal Environments, (in Japanese) (2008).

[22] ISO 7730:2005 Ergonomics of the thermal environment – Analytical determination and interpretation of thermal comfort using calculation of the PMV and PPD indices and local thermal comfort criteria, International Organization for Standardization, 2005.

[23] Mechanisms of Thermal Comfort, The Society of Heating, Air-Conditioning and Sanitary Engineers of Japan, 2006.

[24] M. Ichihara, M. Saitou, M. Nishimura, S. Tanabe, Measurement of convective and radiative heat transfer coefficients of standing and sitting human body by using a thermal mannequin, J. of Architecture, Planning and Environmental Engineering (Transactions of Architectural Institute of Japan) (501) (1997) 45–51, (in Japanese).

[25] C. Rother, V. Kolmogorov, A. Blake, Grabcut: Interactive foreground extraction using iterated graph cuts, ACM Trans. on Graphics 23 (3) (2004) 309–314.

[26] Z. Cao, T. Simon, S.-E. Wei, Y. Sheikh, Realtime multi-person 2d pose estimation using part affinity fields, in: Proceedings of 2017 IEEE Conf. on Computer Vision and Pattern Recognition, 2017.

[27] J.-H. Lee, Y.-K. Kim, K.-S. Kim, S. Kim, Estimating clothing thermal insulation using an infrared camera, Sensors 16 (3).

[28] E. Goceri and E. Dura, Comparison of Weighted K-Means

Clustering Approaches, in: Int. Conf. on Mathematics (ICOMATH2018), An Istanbul Meeting for World Mathematicians, Minisymposium on Approximation Theory & Minisymposium on Math Education, 2018.